

## Insulin-Induced *in Situ* Phosphorylation of the Insulin Receptor Located in the Plasma Membrane versus Endosomes

Bo Wang, Yvonne Balba, and Victoria P. Knutson

*Department of Pharmacology, School of Medicine, University of Texas-Houston, Houston, Texas 77225*

Received August 12, 1996

The binding of insulin to the plasma membrane insulin receptor initiates two dynamic processes: (i) autophosphorylation of the receptor on tyrosine residues, activating the intrinsic tyrosine kinase activity required for insulin signaling, and (ii) endocytosis of the receptor. Recent evidence (Kublaoui *et al.*, *J. Biol. Chem.* **270**, 59–65, 1995) demonstrates that in stimulated adipocytes, the internalized insulin receptor is not only more highly phosphorylated than the receptor remaining on the plasma membrane of the cell, but that IRS-1 binding and phosphorylation also occur in the endosomes. These data suggest that the intracellular insulin receptor mediates insulin action. Utilizing 3T3-L1 adipocytes, we substantiate and extend these findings to document the distribution of receptor between the plasma membrane and the endosomal compartment of insulin-stimulated cells and map the extent and location of the tyrosine phosphorylation sites on the receptor residing in these two cellular locations. We find that following insulin stimulation (i) 90% of the receptor-associated phosphate is located in the endosomal compartment, (ii) the endosomal receptor is most highly phosphorylated in the tyrosine kinase domain, and (iii) significant levels of juxtamembrane domain phosphorylation are detected in the endosomal receptor. These data support the role of the endosomal insulin receptor as the major transducer of insulin action. © 1996 Academic Press, Inc.

The insulin receptor (IR) is a transmembrane glycoprotein composed of 2  $\alpha$  and 2  $\beta$  subunits. The biological effects of insulin are initiated by the binding of insulin to the extracellular  $\alpha$  subunits of the receptor, leading to the autophosphorylation of the intracellular  $\beta$  subunits on specific tyrosine residues. The autophosphorylation is a necessary prerequisite for the activation of the intrinsic tyrosine kinase (TK) activity of the receptor, and this TK activity is required to mediate insulin action (reviewed in 1).

The insulin-induced autophosphorylation sites on the IR  $\beta$  subunit have been mapped to three specific domains: the juxtamembrane domain, the TK domain and the carboxy-terminal cytosolic domain. In the TK domain, three tyrosine residues have been identified as phosphorylation sites: Y1146, Y1150 and Y1151 (2,3). Phosphorylation of these sites leads to activation of the TK activity of the receptor. Maximal TK activity is expressed with the tris-phosphorylated form (4-6). The stimulation of the TK activity of the receptor subsequently leads to the tyrosine phosphorylation of intracellular substrates of the IR, chief among them insulin receptor substrate-1 (IRS-1) (reviewed in 7). Phosphorylated IRS-1 then acts as a docking protein, binding to and activating SH-2 domain-containing proteins in the signaling pathway (8-11). Therefore, phosphorylation of the TK domain is pivotal to the activation of the insulin signaling pathway.

Autophosphorylation in the juxtamembrane domain occurs on residues Y953, Y960 and/or Y972 (2,3). Functionally, the phosphotyrosine residues of this domain of the receptor facilitate the binding of IRS-1 to the IR, thereby permitting the tyrosine phosphorylation of IRS-1 by

Abbreviations: DNP, dinitrophenyl; FBS, fetal bovine serum; IR, insulin receptor; PBS, phosphate-buffered saline; TBS, Tris-buffered saline; SDS–PAGE, sodium dodecyl sulfate polyacrylamide gel electrophoresis; PM, plasma membrane; DMEM, Dulbecco's modified Eagle's media; TLC, thin layer chromatography; TK, tyrosine kinase.

the TK activity of the IR (12,13). Autophosphorylation of the cytosolic tail domain occurs on residues Y1316 and Y1322 (2,3). While this domain has been implicated in the mitogenic response induced by insulin (14,15), recently it has been demonstrated that the regulatory subunit of phosphatidylinositol 3-kinase (PI 3-kinase) binds directly to this phosphorylated domain of the IR, leading to direct activation of the enzyme (16).

Occurring simultaneously with autophosphorylation and receptor activation, the IR located at the plasma membrane (PM) of the cell undergoes endocytosis (17). Site-directed mutagenesis and domain deletion studies have demonstrated that this endocytic process requires the TK activity of the receptor (18), as well as an intact juxtamembrane domain (19). Previous studies have demonstrated that the receptor located in the cellular endosomes is more highly phosphorylated than the receptor located in the PM, and the intracellular receptor can phosphorylate exogenous substrates (20-22). In addition, a recent study demonstrated that in insulin-stimulated adipocytes, 20% of the total cellular IRS-1 was associated with a light microsomal fraction, and that the level of phosphorylation of IRS-1 in this fraction mirrored the phosphorylation state of the intracellular receptor (20). These data suggest that the intracellular receptor plays a role in insulin signal transmission.

While the multiple studies cited above have now documented that the intracellular receptor is more highly phosphorylated than the receptor located at the PM, it has not been documented which tyrosine residues of the receptor are phosphorylated (or dephosphorylated) as the receptor migrates from one cellular address to the other. Since the phosphorylation status of the 3 domains of the receptor regulate TK activity and the ability of the receptor to interact with docking molecules, understanding which tyrosine residues of the endosomal receptor are phosphorylated would provide insight into the signaling pathways which are activated by the endosomal receptor. Consequently, the studies described in this report were undertaken to map the phosphorylated tyrosine residues of the IR located in the PM and endosomal fraction of insulin-stimulated cells.

## MATERIALS AND METHODS

**Materials.** Cell culture media and sera were obtained from JRH Scientific (Lenexa, KS), and Falcon tissue culture plastic was purchased from Becton Dickinson (Bedford, MA). Insulin was obtained from Elanco (Eli Lilly, Indianapolis, IN). Cellulose acetate thin layer chromatography (TLC) plates were obtained from Eastman Kodak Company (Rochester, NY).  $^{32}\text{P}$ -orthophosphate, 3000 Ci/mmol, was obtained from ICN (Costa Mesa, CA), and carrier-free  $\text{Na}^{125}\text{I}$  was obtained from Amersham (Arlington Heights, IL). Reagents for sodium dodecylsulfate polyacrylamide gel electrophoresis (SDS-PAGE) were obtained from BioRad (Hercules, CA). Proteinase inhibitors were purchased from Calbiochem (LaJolla, CA). Buffers, salts and analytical grade solvents were obtained from common supply houses.

**Cell culture.** 3T3-L1 adipocytes were grown as previously described (23,24). The adipocytes were insulin-free for 8-10 days prior to use, and the culture media was changed 18-24 h before the cells were used in an experiment.

**Metabolic labeling and 2-dimensional phosphopeptide mapping.** Fully-differentiated, insulin-free 3T3-L1 adipocyte monolayers in 100 mm dishes were incubated with 3 ml of phosphate-free DMEM containing 10% dialyzed, phosphate-free FBS and 1 mCi  $^{32}\text{P}$ -orthophosphate for 3 h. During the final 45 min of this incubation period, 1.7  $\mu\text{M}$  insulin, or buffer alone, was added to the cells. All subsequent steps were performed at 4°C. The culture medium was aspirated from the monolayers and the adipocytes were washed with TBS, and scraped from the dishes into lysis buffer (5 mM imidazole, pH 7.4, containing 250 mM sucrose, 1  $\mu\text{g}/\text{ml}$  chymostatin, 1  $\mu\text{g}/\text{ml}$  pepstatin, 1  $\mu\text{g}/\text{ml}$  leupeptin, 2  $\mu\text{g}/\text{ml}$  antipain, 10  $\mu\text{g}/\text{ml}$  benzamidin, 10  $\mu\text{M}$  EDTA, 0.2 mM phenylmethylsulfonyl fluoride, 5  $\mu\text{g}/\text{ml}$  E-64, 1  $\mu\text{g}/\text{ml}$  sodium vanadate and 17 mM sodium molybdate). The endosomal and PM fractions were prepared as previously described (22,25). The IR was extracted from the PM and endosomal fractions by incubation with extraction buffer (50 mM Tris, pH 7.4, containing proteinase inhibitors and phosphatase inhibitors, and 4% Triton X-100) for 1 h at 4°C. The insoluble material was removed by centrifugation, and the membrane extracts were subjected to SDS-PAGE on 7.5% resolving polyacrylamide gels. The wet gels were exposed to X-ray film for 1 h to visualize the  $\beta$  subunit of the IR at 92 kDa. The  $\beta$  subunit band was excised from the gel, and cut into small pieces.

Elution of the protein from the gels, tryptic digestion and 2-dimensional phosphopeptide analysis was performed as previously described (2,3). The recovery of radioactivity from the gel slices averaged 92-98%. Radioactivity on the developed TLC plate was visualized and quantitated directly on a Betascope model 603 Blot Analyzer (Betagen,

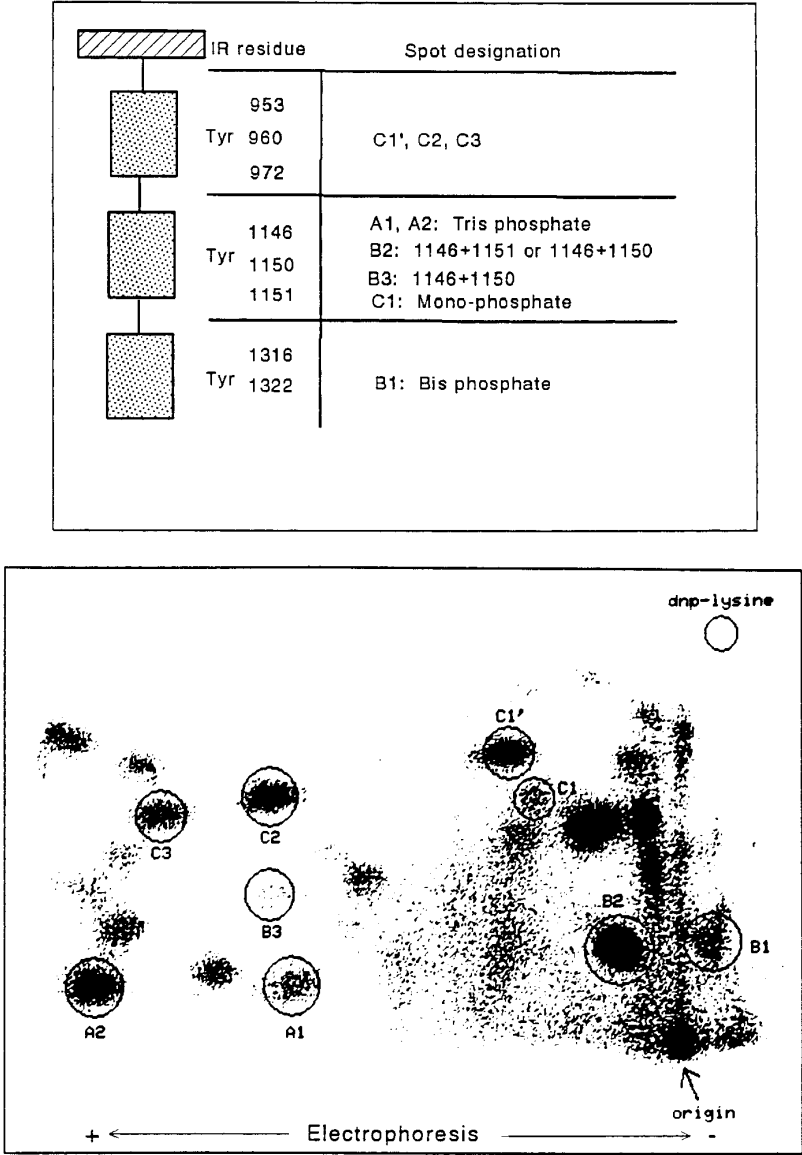


**FIG. 1.** Schematic representation of the autophosphorylation domains of the  $\beta$  subunit of the IR and representative two-dimensional phosphopeptide map of the receptor. **(A)** Tyrosine residues of the  $\beta$  subunit of the IR which are phosphorylated in response to insulin binding, and the designation of the tryptic phosphopeptide spots which correspond to the phosphorylated domains. Assignments are taken from Tavare, et al (2,3). **(B)** A representative two-dimensional tryptic phosphopeptide map of the  $\beta$  subunit of the IR obtained from receptor located in the endosomes of insulin-stimulated 3T3-L1 adipocytes. The circled spots are designated as shown in A. The origin is indicated by the arrow, and the open circle in the upper right corner indicates the migration of the marker DNP-lysine.

ATC Diagnostics, Inc, Framingham, MA), or the spots were excised from the plate and subjected to scintillation counting. Comparable results were obtained with the two techniques.

Figure 1A illustrates the 3 domains of the IR which are phosphorylated in response to insulin binding, and the assignments and spot designation determined by Tavare et al. (2,3). Tyrosine residues 953, 960 and 972 reside in the juxtamembrane domain of the receptor, the TK (or regulatory) domain contains tyrosine residues 1146, 1150 and 1151, and the carboxy-terminal domain contains tyrosine residues 1316 and 1322. Figure 1B is a representative 2D

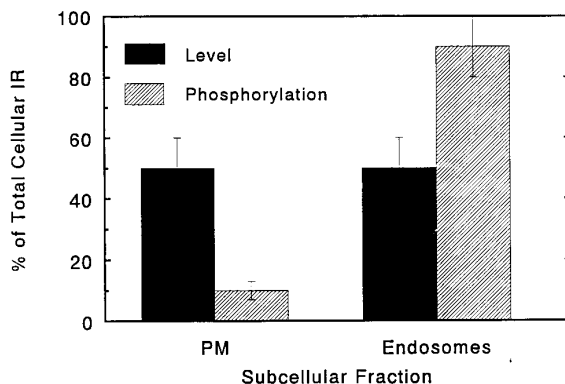


**FIG. 2.** Comparison of the distribution of IR protein and  $^{32}\text{P}$  incorporation into the  $\beta$  subunit of the IR isolated from the PM or endosomal fraction of insulin-stimulated 3T3-L1 adipocytes. IR protein (solid bars) was determined either by insulin binding activity or by immunoblot analysis utilizing an antibody specific for the  $\beta$  subunit of the IR.  $\beta$  subunit phosphorylation (hatched bars) was quantitated by excising the subunit from SDS-PAGE gels and quantitating the incorporated radioactivity by Cherenkov counting.

phosphopeptide map obtained from the endosomal fraction of insulin stimulated cells, demonstrating the relative locations of all of the phosphopeptide spots described in Figure 1A, plus indicating the locations of the origin and the dye marker DNP-lysine. For purposes of quantitative presentation, radioactivity associated with the individual spots of a given domain were summed together, to present the phosphorylation of a specific domain. Thus, the sum of the radioactivity found in spots C1', C2 and C3 represents the phosphorylation state of the juxtamembrane domain; the total radioactivity found in spots A1, A2, B2, B3 plus C1 represents the phosphorylation state of the TK domain; the radioactivity associated with spot B1 represents the phosphorylation state of the carboxy-terminal domain. To further dissect the phosphorylation state of the TK domain, the level of tris-phosphorylation of this domain was determined by the sum of the radioactivity present in spots A1 and A2. Bis-phosphorylation was quantitated by summing spots B2 and B3, and the radioactivity in spot C1 was the mono-phosphate form of this domain.

As is apparent in Figure 1B, some radioactivity remains at the origin of the developed thin layer chromatogram. This is presumably due to incompletely digested  $\beta$  subunit, which, if present at high enough levels, could lead to a biased distribution of resolved phosphopeptides. To minimize this potential artifact, in all of the results reported here, less than 15% of the total radioactivity applied to the TLC plate remained at the origin after 2D analysis.

**Immunoblot analysis.** To quantitate the amount of IR obtained in the PM and endosomal fractions, the detergent extracts were subjected to immunoblot analysis as previously described (26) utilizing an affinity-purified polyclonal anti-peptide antibody against the carboxy-terminus of the insulin receptor  $\beta$  subunit. Band intensities were quantitated by densitometry.

**Insulin binding assay.** Insulin was iodinated as previously described (27).  $^{125}\text{I}$ -insulin binding to solubilized insulin receptor was determined as previously described (27). Total binding was determined at a final  $^{125}\text{I}$ -insulin concentration of 15 nM. Non-specific binding was determined with 15 nM  $^{125}\text{I}$ -insulin and 1  $\mu\text{M}$  unlabeled insulin. Specific binding was calculated as the difference between total and non-specific binding.

## RESULTS

Following stimulation of the 3T3-L1 adipocytes with a saturating concentration of insulin for 45 min (the time required to attain steady-state levels of IR within the endosomes (28)), the amount of IR protein and the level of radioactive phosphate incorporated into the receptor located in the PM fraction and the endosomal fraction were determined. The results are shown in Figure 2. The amount of IR located in the two fractions was determined by two separate methods: insulin binding activity, which quantitates the level of functional insulin-binding  $\alpha$  subunit, and immunoblot analysis with an antibody which specifically detects the  $\beta$  subunit of the receptor. Both methods of analysis yielded quantitatively similar results, in that 50% of the total cellular IR resided in the PM and 50% of the receptor was detected in the endosomal fraction of insulin stimulated cells. Quantitation of the incorporation of radioactive phosphate into the IR of these two subcellular fractions demonstrated that only 10% of the  $^{32}\text{P}$  was

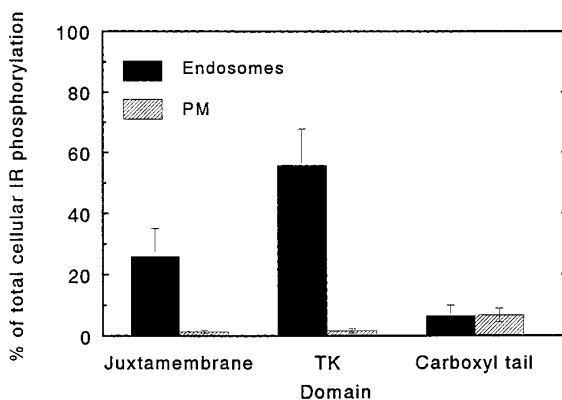


**FIG. 3.** The insulin-induced phosphorylation pattern of the IR in the endosomes (solid bars) and PM (hatched bars) of the whole cell. Distribution of  $^{32}\text{P}$  between the juxtamembrane, TK and carboxyl tail domains of the  $\beta$  subunit of the IR. The 100% level represents the total level of phosphorylation of the IR. The error bars represent the SD.

incorporated into the receptor located in the PM, while the remaining 90% of the phosphate resided in the IR found in the endosomal compartment. These results demonstrate that while the receptor is equally distributed between the PM and the endosomes, there is 9-fold more  $^{32}\text{P}$  associated with the receptor found in the endosomal compartment than is found in the PM receptor.

To determine the location of the tyrosine residues in the IR  $\beta$  subunit which are phosphorylated in response to insulin stimulation of the intact adipose cell, and to determine the relative level to which these residues are phosphorylated, the phosphorylated receptor isolated from the PM or endosomal fraction was subjected to 2D phosphopeptide mapping. The phosphopeptide spots were analyzed and quantitated as described in "Methods" to facilitate characterization of the phosphorylation of the juxtamembrane domain, the TK domain and the carboxyl tail domain of the receptor in either the PM or endosomal fraction. Figure 3 illustrates the results which are derived from 9 separate experiments. Receptor isolated from the PM was poorly phosphorylated. Less than 2% of the total cellular receptor phosphorylation was found in the juxtamembrane or TK domain of the PM receptor, while 6.7% of the total receptor phosphorylation was found in the carboxyl tail domain of the IR within the PM. Interestingly, this profile is essentially identical to the distribution of radioactivity found in the PM receptor from basal, non-insulin-stimulated adipocytes (data not shown). In contrast, the IR located in the endosomes was highly phosphorylated. Nearly 56% of the total cellular IR phosphorylation was found within the TK domain of the endosomal receptor, and 26% was found within the juxtamembrane domain. The carboxyl tail domain of the endosomal IR was phosphorylated to the same extent as the carboxyl tail domain of the IR within the PM.

To further characterize the distribution of the tyrosine phosphate within the TK domain, this domain was further analyzed to quantitate the level of mono-, bis- and tris-phosphorylation. This characterization is shown in Table 1. The TK domain of the receptor isolated from the PM of insulin-stimulated cells demonstrated a total lack of tris-phosphate. This result was confirmed in 9 separate experiments. Mono- and bis-phosphorylated receptor was detected in a relative ratio of 1:2. The TK domain of the receptor isolated from the endosomes of insulin-stimulated cells demonstrated a high level of bis- and tris-phosphorylation, with a barely-detectable level of mono-phosphorylation. These data indicate that not only is there more tyrosine phosphorylation in the TK domain of the endosomal insulin receptor compared to the PM receptor, but that within this domain of the endosomal receptor, most of the phosphate is found in the more catalytically active bis- and tris-phosphorylated form.

TABLE 1  
Level of Phosphorylation within the Tyrosine Kinase Domain of  
the Insulin Receptor Isolated from Plasma Membrane or Endosomes  
of Insulin-Stimulated 3T3-L1 Adipocytes

Degree of phosphorylation	Plasma membrane	Endosomes
Mono	0.54 ± 0.13%	2.5 ± 1.1%
Bis	1.18 ± 0.43%	21.1 ± 10.4%
Tris	0	29.0 ± 11.9%

*Note.* Values are expressed as percentage of total cellular insulin  
receptor phosphorylation ± SD. *n* = 9.

DISCUSSION

The results presented above indicate that upon insulin stimulation of 3T3-L1 adipocytes, not only is the level of phosphorylation of the endosomal IR 9-fold greater than the level of phosphorylation of the receptor located in the PM, but that the distribution of phosphate between the three domains of the  $\beta$  subunit of the endosomal versus PM receptor is distinctly and significantly different. Receptor from the PM demonstrates very little phosphorylation in the juxtamembrane or TK domain. In view of the importance of the phosphorylated juxtamembrane domain in interacting with IRS-1 (12,13), the receptor located in the PM would be predicted to bind very little IRS-1, and correspondingly promote insulin signal transduction via IRS-1-mediated pathways to a minimal extent. The TK domain of the PM receptor also demonstrates a low level of tyrosine phosphorylation, and of that low level, only the low activity mono- and bis-phosphorylation state could be found. The low level phosphorylation in this domain would also contribute to a low efficiency signal transduction capacity of the IR, since the TK activity of the receptor is required for the phosphorylation of substrates, such as IRS-1, leading to the propagation of the insulin signal (7). Thus, based on the phosphorylation profile of both the juxtamembrane and TK domains, the IR located in the PM would be predicted to be a poor mediator of the insulin signal.

In contrast, the IR located in the endosomes of insulin-stimulated cells is highly phosphorylated at both the juxtamembrane domain and the TK domain. The phosphorylated state of the juxtamembrane domain would be predicted to promote the association between IRS-1 and the endosomal IR, and other investigators have, in fact, found this to be the case in insulin-stimulated adipose cells (20). The high level of phosphorylation in the TK domain, especially the high level of bis- and tris-phosphorylation, would be predicted to lead to a high level of TK activity of the endosomal receptor, leading to a high level of IRS-1 phosphorylation. Again, others have documented that the TK activity of the endosomal IR is higher than that found with the PM receptor, and that IRS-1 phosphorylation paralleled the phosphorylation state of the endosomal receptor (20).

These data strongly support a role of the endosomal insulin receptor in insulin signal transduction.

It is interesting to note that the phosphorylation state of the carboxyl tail domain of the receptor does not change as the receptor migrates from the PM to the endosomes. In addition, our data also indicate that in the basal, non-insulin-stimulated state, the same low level carboxyl tail phosphorylation is also detected (data not shown). Phosphorylation of this domain under *in situ* conditions has recently been shown to facilitate a direct interaction between the insulin receptor and p85, the regulatory subunit of PI 3-kinase, leading to activation of PI 3-kinase (16). Earlier reports, however, demonstrated that p85 binds to phosphorylated IRS-1, leading

to PI 3-kinase activation (29). IRS-1 phosphorylation is mediated through binding to the phosphorylated juxtamembrane domain, and the phosphorylation of IRS-1 occurs by the active TK of the receptor. Since we have found a high level of juxtamembrane and TK domain phosphorylation in the endosomal IR from insulin-stimulated cells, but low levels of carboxyl tail phosphorylation, it would seem most likely that the majority of cellular PI 3-kinase would be activated through its interaction with IRS-1 within the endosomal compartment and less likely that a large proportion of PI 3-kinase would be activated through direct interaction with the poorly phosphorylated carboxyl tail domain of the receptor. Nevertheless, in NIH-3T3 cells overexpressing the IR, Levy-Toledano et al. demonstrated that more p85 co-immunoprecipitated with the IR than with IRS-1 (16). However, it is possible that the p85 detected in the receptor immunoprecipitates in this study was associated with the IR through an interaction bridged by IRS-1 and not a direct association between the IR and p85. Therefore, these data may be misleading. Also, these investigators did not detect any association of p85 with the IR in non-insulin-stimulated cells. Based on our findings that the level of carboxyl tail phosphorylation is the same in basal and stimulated cells, our data would predict a comparable direct association between p85 and the receptor in the absence or presence of insulin. Experiments to pursue these predictions are currently underway.

Previous investigators have demonstrated a role of the carboxyl tail domain of the receptor in mitogenic signalling (14,15). No direct role for phosphorylation of this domain has been defined in this signaling pathway, and we detect no change in the phosphorylation state of this domain when comparing the basal cell receptor with the receptor localized in the PM or endosomes of insulin-stimulated cells. However, in our experiments, the adipocytes were treated with insulin for only 45 min, whereas insulin treatment times of 36-48 h are utilized in measuring mitogenesis. This suggests that carboxyl tail phosphorylation may be modified upon chronic stimulation of the cell with insulin. We are currently pursuing studies to evaluate the effect of chronic insulin treatment on the phosphorylation state of the IR, with emphasis on the carboxyl tail domain.

In summary, these studies demonstrate that upon stimulation with insulin, the endosomal IR contains 9-fold more tyrosine phosphate than the receptor located in the PM. The endosomal receptor contains a high level of phosphorylation in the TK domain, particularly in the bis- and tris-phosphorylated forms which have been found to be the forms of this domain which lead to the highest levels of TK activity. The juxtamembrane domain of the endosomal receptor is also highly phosphorylated, providing the appropriate form for binding to IRS-1. In contrast, the IR residing at the PM of insulin stimulated cells has a nearly undetectable level of phosphorylation in the TK domain and the juxtamembrane domain. These data suggest that the IR located in the endosomal fraction of the insulin-stimulated cell is in the phosphorylation state most favorable to mediate insulin signalling.

#### ACKNOWLEDGMENT

This work was supported by grant IBN9220174 from the National Science Foundation.

#### REFERENCES

1. White, M. F., and Kahn, C. R. (1994) *J. Biol. Chem.* **269**, 1-4.
2. Tavaré, J. M., and Denton, R. M. (1988) *Biochem. J.* **252**, 607-615.
3. Tavaré, J. M., Clack, B., and Ellis, L. (1991) *J. Biol. Chem.* **266**, 1390-1395.
4. Flores-Riveros, J. R., Sibley, E., Kastelic, T., and Lane, M. D. (1989) *J. Biol. Chem.* **264**, 21557-21572.
5. Wilden, P. A., Siddle, K., Haring, E., Backer, J. M., White, M. F., and Kahn, C. R. (1992) *J. Biol. Chem.* **267**, 13719-13727.
6. White, M. F., Shoelson, S. E., Keutmann, H., and Kahn, C. R. (1988) *J. Biol. Chem.* **263**, 2969-2980.
7. Myers, M. G., and White, M. R. (1993) *Diabetes* **42**, 643-650.
8. Kahn, C. R. (1994) *Diabetes* **43**, 1066-1084.

9. Shoelson, S. E., Sivaraja, M., Williams, K. P., Hu, P., Schlessinger, J., and Weiss, M. A. (1993) *EMBO Journal* **12**, 795–802.
10. Ando, A., Yonezawa, K., Gout, I., Nakata, T., Ueda, H., Hara, K., Kitamura, Y., Noda, Y., Takenawa, T., and Hirokawa, N. (1994) *EMBO J.* **13**, 3033–3038.
11. Case, R. D., Piccione, E., Wolf, G., Benett, A. M., Lechleider, R. J., Neel, B. G., and Shoelson, S. E. (1994) *J. Biol. Chem.* **269**, 10467–10474.
12. Murakami, M. S., and Rosen, O. M. (1991) *J. Biol. Chem.* **266**, 22653–22660.
13. White, M. F., Livingston, J. N., Backer, J. M., Lauris, V., Dull, T. J., Ullrich, A., and Kahn, C. R. (1988) *Cell* **54**, 641–649.
14. Ando, A., Momomura, K., Tobe, K., Yamamoto-Honda, R., Sakura, H., Tamori, Y., Kaburagi, Y., Koshio, O., Akanuma, Y., Yazaki, Y., Kasuga, M., and Kadowaki, T. (1992) *J. Biol. Chem.* **267**, 12788–12796.
15. Pang, L., Milarski, K. L., Ohmichi, M., Takata, Y., Olefsky, J. M., and Saltiel, A. R. (1994) *J. Biol. Chem.* **269**, 10604–10608.
16. Levy-Toledano, R., Taouis, M., Blaettler, D. H., Gorden, P., and Taylor, S. I. (1994) *J. Biol. Chem.* **269**, 31178–31182.
17. Knutson, V. P. (1991) *FASEB J.* **5**, 2130–2138.
18. McClain, D. A., Maegawa, H., Lee, J., Dull, T. J., Ullrich, A., and Olefsky, J. M. (1987) *J. Biol. Chem.* **262**, 14663–14671.
19. Backer, J. M., Shoelson, S. E., Haring, E., and White, M. F. (1991) *J. Cell Biol.* **115**, 1535–1545.
20. Kublaoui, B., Lee, J., and Pilch, P. F. (1995) *J. Biol. Chem.* **270**, 59–65.
21. Khan, M. N., Baquiran, G., Brule, C., Burgess, J., Foster, B., Bergeron, J. J. M., and Posner, B. I. (1989) *J. Biol. Chem.* **264**, 12931–12940.
22. Khan, M. N., Savoie, S., Bergeron, J. J. M., and Posner, B. I. (1986) *J. Biol. Chem.* **261**, 8462–8472.
23. Knutson, V. P. (1986) *J. Biol. Chem.* **261**, 10306–10312.
24. Laemmli, U. K. (1970) *Nature* **227**, 680–685.
25. Hubbard, A. L., Wall, D. A., and Ma, A. (1983) *J. Cell Biol.* **96**, 217–229.
26. Knutson, V. P., and Buck, R. A. (1991) *Arch. Biochem. Biophys.* **285**, 197–204.
27. Knutson, V. P., Ronnett, G. V., and Lane, M. D. (1982) *Proc. Natl. Acad. Sci. USA* **79**, 2822–2826.
28. Knutson, V. P., Ronnett, G. V., and Lane, M. D. (1983) *J. Biol. Chem.* **258**, 12139–12142.
29. Giorgetti, S., Ballotti, R., Kowalski-Chauvel, A., Tartare, S., and Van Obberghen, E. (1993) *J. Biol. Chem.* **268**, 7358–7364.